Liver Glutamate Dehydrogenase Controls Whole-Body Energy Partitioning Through Amino Acid-Derived Gluconeogenesis and Ammonia Homeostasis

Karaca Emre, Melis; Martin-Levilain, Juliette; Grimaldi, Mariagrazia; Li, Lingzi; Dizin, Eva; Emre, Yalin; Maechler, Pierre

How to cite

KARACA EMRE, Melis et al. Liver Glutamate Dehydrogenase Controls Whole-Body Energy Partitioning Through Amino Acid-Derived Gluconeogenesis and Ammonia Homeostasis. In: Diabetes, 2018, vol. 67, n° 10, p. 1949–1961. doi: 10.2337/db17-1561

This publication URL: https://archive-ouverte.unige.ch/unige:110984

Publication DOI: 10.2337/db17-1561

Liver Glutamate Dehydrogenase Controls Whole-Body Energy Partitioning Through Amino Acid–Derived Gluconeogenesis and Ammonia Homeostasis

Melis Karaca,[1,2] Juliette Martin-Levilain,[1,2] Mariagrazia Grimaldi,[1,2] Lingzi Li,[1,2] Eva Dizin,[1] Yalin Emre,[3] and Pierre Maechler[1,2]

Diabetes 2018;67:1949–1961 | https://doi.org/10.2337/db17-1561

Ammonia detoxification and gluconeogenesis are major hepatic functions mutually connected through amino acid metabolism. The liver is rich in glutamate dehydrogenase (GDH) that catalyzes the reversible oxidative deamination of glutamate to α-ketoglutarate and ammonia, thus bridging amino acid–to–glucose pathways. Here we generated inducible liver-specific GDH-knockout mice (Hep*Glud1*$^{-/-}$) to explore the role of hepatic GDH on metabolic homeostasis. Investigation of nitrogen metabolism revealed altered ammonia homeostasis in Hep*Glud1*$^{-/-}$ mice characterized by increased circulating ammonia associated with reduced detoxification process into urea. The abrogation of hepatic GDH also modified energy homeostasis. In the fasting state, Hep*Glud1*$^{-/-}$ mice could barely produce glucose in response to alanine due to impaired liver gluconeogenesis. Compared with control mice, lipid consumption in Hep*Glud1*$^{-/-}$ mice was favored over carbohydrates as a compensatory energy fuel. The changes in energy partitioning induced by the lack of liver GDH modified the circadian rhythm of food intake. Overall, this study demonstrates the central role of hepatic GDH as a major regulator for the maintenance of ammonia and whole-body energy homeostasis.

The turnover of amino acids is characterized by the respective metabolisms of nitrogen and carbon skeletons. The crucial steps for nitrogen metabolism are first, the removal of the amino group in the form of ammonia (NH_3), and second, its detoxification into urea to prevent further accumulation of the neurotoxic ammonium (NH_4^+). The liver is the central organ of ammonia metabolism, and the muscles and kidneys play a role in the interorgan exchange and final ammonia disposal (1,2). The liver has a remarkable capacity to remove ammonia via the high-capacity/low-affinity urea cycle as well as low-capacity/high-affinity glutamine synthetase (GS) (3). Both of these ammonia-removal systems engage glutamate as an intermediary metabolite.

Glutamine serves, along with alanine, as a major nontoxic interorgan ammonia shuttle in the body (2,4). Glutamine is deamidated to glutamate by glutaminase (GLS), thereby generating ammonia. Alanine aminotransferase (ALAT) catalyzes the transfer of an amino group from the donor alanine to the acceptor α-ketoglutarate (α-KG), thereby producing pyruvate and glutamate. Then, glutamate is deaminated to α-KG through glutamate dehydrogenase (GDH), releasing NH_3 for urea synthesis. GDH is abundant in the liver and is the only mammalian enzyme that catalyzes the deamination of an amino acid. Despite its specificity for glutamate, GDH, via the coupling to aminotransferase reactions, plays a key role in the deamination of most amino acids.

Beside its role in nitrogen metabolism, the liver is also the major site for gluconeogenesis, which is a fundamental process under metabolic-challenging conditions, such as fasting or sustained physical exercise (5–9). Primary carbon skeletons used for gluconeogenesis may derive from pyruvate, lactate, glycerol, and amino acids. During fasting, glutamine and alanine account for 60–80% of the amino

[1]Department of Cell Physiology and Metabolism, University of Geneva Medical School, Geneva, Switzerland
[2]Faculty Diabetes Center, University of Geneva Medical School, Geneva, Switzerland
[3]Department of Pathology and Immunology, University of Geneva Medical School, Geneva, Switzerland

Corresponding authors: Melis Karaca, meliskaraca@gmail.com, and Pierre Maechler, pierre.maechler@unige.ch.

Received 21 December 2017 and accepted 1 July 2018.

This article contains Supplementary Data online at http://diabetes.diabetesjournals.org/lookup/suppl/doi:10.2337/db17-1561/-/DC1.

acids released from the skeletal muscles and subsequently taken up by the liver (10). GDH represents an essential link between amino acids and carbohydrates, channeling the carbon skeletons of several amino acids into the tricarboxylic acid cycle for anaplerosis and the provision of gluconeogenic substrates (2,11,12). The importance of GDH activity is witnessed by the severity of disorders where GDH function is altered (gain of function mutations), such as hyperinsulinism/hyperammonemia syndrome (13,14).

Although our current knowledge points to liver GDH as a key player in nitrogen metabolism and amino acid–derived gluconeogenesis, no study has challenged yet such an assumption by in vivo abrogation of GDH in hepatocytes. Here, we generated inducible liver-specific GDH-knockout mice to investigate the role of liver GDH in metabolic homeostasis under basal and energy-challenging conditions. We found that hepatic GDH was critical for maintenance of ammonia and urea homeostasis, playing a central role in the circadian rhythm of food intake and energy partitioning through alanine-induced gluconeogenesis.

RESEARCH DESIGN AND METHODS

Mice

Glud1 floxed (*Glud1*$^{lox/lox}$) mice (*Glud1*$^{tm1.1Pma}$, MGI:3835667 [15]) were crossed with mice carrying the tamoxifen-dependent Cre-ER^{T2} recombinase coding sequence preceded by an internal ribosomal entry site inserted in the 3′-untranslated region of the serum albumin gene (16). The in vivo deletion of GDH in hepatocytes (Hep*Glud1*$^{-/-}$ mice) was induced at 8 weeks of age by subcutaneous implantation of tamoxifen pellets (Tamoxifen free base, 25 mg/pellet, 21-day release, E-361; Innovative Research of America) in male *Glud1*$^{lox/lox}$ mice carrying the albumin–Cre-ER^{T2} construct and used for analyses 4 weeks later at 12 weeks of age, unless otherwise specified. Animals were maintained on a mixed (C57BL/6J × 129/Sv) genetic background to avoid inbred strain-specific phenotypes. As control mice, we used *Glud1*$^{lox/lox}$ littermates to optimize standardization of the genetic background between the two groups. To rule out the possibility that the albumin-*Cre* transgene used in the current study may have independently contributed to the metabolic phenotype, we studied in parallel cohorts of mice carrying the albumin-*Cre* transgene without floxed *Glud1* littermates to investigate some metabolic parameters, revealing no effects of Albumin-*Cre* per se. Mice were maintained in our certified animal facility (12-h × 12-h light/dark cycle with 7 A.M. on and 7 P.M. off) according to procedures that were approved by the animal care and experimentation authorities of the Canton of Geneva (#1034-3615-1R).

Expression by Immunoblotting and Immunofluorescence

Antibodies against GDH (100-4158; Rockland), actin (MAB1501; Millipore), glutaminase (ab200408; Abcam), porin (ab34726; Abcam), G6Pase (developed by Dr. G. Mithieux's laboratory, INSERM U855, Lyon, France), and PEPCK-c (ab70358; Abcam) were used for immunoblotting experiments on whole-tissue extracts. For immunofluorescence, tissue sections were stained using antibodies against GDH and glutamine synthetase (MAB302; Millipore) and bodipy dye (D3922; Molecular Probes) for lipid droplets. Primary hepatocytes were labeled with MitoTracker Orange CMTMRos (M-7510; Molecular Probes) to visualize mitochondria. Nuclei were stained with DAPI or Hoechst (Molecular Probes). Detailed protocols are described in the Supplementary Experimental Procedures.

GDH Enzymatic Activity

GDH enzymatic activity was measured in tissues collected in ice-cold saline before homogenization in 50 mmol/L Tris/HCl (pH 7.4), 0.5 mmol/L EDTA, and 1 mmol/L β-mercaptoethanol in glass potter. After 40-min centrifugation at 8,000*g*, supernatants were assayed for enzymatic activity as previously described (17).

Determination of Metabolic Parameters

Blood, urine, and tissue parameters were determined on samples collected from animals fed or fasted overnight (O/N) for 18 h (from 4 P.M. to 10 A.M.). Specific measurements are described in detail in the Supplementary Experimental Procedures.

In Vivo Experiments

Body composition was assessed by an EchoMRI-700 quantitative nuclear magnetic resonance analyzer (Echo Medical Systems, Houston, TX). Metabolic parameters and physical activity were measured using a LabMaster system (TSE Systems GmbH, Bad Homburg, Germany) at the Small Animal Phenotyping Core Facility (University of Geneva, Geneva, Switzerland) under controlled temperature (22 ± 1°C) and lighting (light on: 0700–1900 h). Energy expenditure and respiratory exchange ratio (RER) were determined by indirect calorimetry, locomotor activity was recorded by an infrared frame, and food and water intake were measured by highly sensitive feeding and drinking sensors. These parameters were measured in mice housed individually in LabMaster metabolic cages (TSE Systems GmbH).

Glucose and insulin tolerance tests were performed upon i.p. injection of D-glucose (2 g/kg; Sigma-Aldrich) after an O/N fast or insulin (0.75 units/kg; NovoRapid, Novo Nordisk) on fed mice. Glycerol, pyruvate, alanine, and glutamine challenge tests were performed upon i.p. injection of glycerol (2 g/kg; Sigma-Aldrich), sodium pyruvate (2 g/kg; Sigma-Aldrich), L-arginine (2 g/kg; Sigma-Aldrich), or L-glutamine (2 g/kg; Acros Organics) after an O/N fast. For ammonia and urea determination, blood was taken from mice under anesthesia from the abdominal aorta and portal, hepatic, and renal veins. Detailed procedures are given in the Supplementary Experimental Procedures.

Glucose Production by Primary Hepatocytes and Renal Proximal Tubule Cells

Primary hepatocytes were starved for 6 h in DMEM 5030 (without glucose, glutamine, and pyruvate; Sigma-Aldrich) for glycogen depletion. The medium was replaced by Krebs-Ringer bicarbonate HEPES (KRBH) buffer (140 mmol/L NaCl, 3.6 mmol/L KCl, 0.5 mmol/L NaH_2PO_4, 0.5 mmol/L $MgSO_4$, 2 mmol/L $NaHCO_3$, 1.5 mmol/L $CaCl_2$, and 10 mmol/L HEPES) alone (for basal condition) or KRBH containing 20 mmol/L alanine or 10 mmol/L glutamine (for stimulatory conditions). Cells were further incubated for 60 min in a water bath at 37°C. The supernatant was stored at −20°C until assayed for glucose. Renal cells (200×10^3) were preincubated for 30 min at 37°C in silicone-coated glass tubes gassed with a mixture of O_2:CO_2 (95%:5%), in a shaking water bath containing KRBH buffer. Thereafter, the medium was replaced by 500 μL KRBH containing 20 mmol/L alanine or 10 mmol/L glutamine. Cells were further incubated for 60 min at 37°C. The supernatant was stored at −20°C until assayed for glucose.

Statistics

Data are presented as means ± SEM. Statistical analyses were performed using GraphPad Prism 6 software, with one-way ANOVA when more than two groups of data were compared and with the two-tailed Student *t* test when only two groups of data were concerned. We deemed the difference being significant at $P < 0.05$.

RESULTS

Assessment of Liver-Specific GDH-Knockout Mouse, Hep*Glud1*$^{-/-}$

The in vivo deletion of GDH in hepatocytes was induced at 8 weeks of age by subcutaneous implantation of tamoxifen pellets in *Glud1*$^{lox/lox}$ mice carrying the *Alb-CreERT2* construct, giving rise to liver-specific GDH-knockout mice (Hep*Glud1*$^{-/-}$) (Supplementary Fig. 1*A*). Four weeks after in vivo induction of recombination by tamoxifen, deletion was successful and specific for the liver of Hep*Glud1*$^{-/-}$ mice (<5% remaining of immunoreactive GDH), GDH protein being preserved in nonhepatic tissues normally expressing the *Glud1* gene (Fig. 1*A* and Supplementary Fig. 1*B*). Immunofluorescence of liver sections confirmed the deletion of GDH in Hep*Glud1*$^{-/-}$ hepatocytes (Fig. 1*B* and Supplementary Fig. 1*C*). Accordingly, GDH enzymatic activity was deficient in liver homogenates of Hep*Glud1*$^{-/-}$ mice (−98%, $P < 0.01$) (Fig. 1*C*). Expression of liver GDH was absent at least up to 50 weeks after tamoxifen implantation (Supplementary Fig. 1*D*). GDH ablation altered neither the liver morphology nor the liver-to-body weight ratio of young and aged Hep*Glud1*$^{-/-}$ mice (Supplementary Fig. 2). Intracellular lipid distribution and mitochondrial morphology were not modified by the hepatocyte-specific GDH deletion (Supplementary Fig. 3). Finally, plasma levels of ALAT and aspartate aminotransferase (ASAT), measured as an index of the global liver health status, did not show differences between control *Glud1*$^{lox/lox}$ and knockout Hep*Glud1*$^{-/-}$ mice (Supplementary Table 1).

Liver GDH Controls Ammonia Detoxification Into Urea

We next examined the role of GDH in the fate of cellular ammonia by quantifying circulating ammonia levels in the fed animals at different sites of the vasculature. Blood was collected from the same animal from the portal vein (representing the "intestinal outflow" and ~85% of the "liver inflow"), the abdominal aorta (representing the remaining 15% of the "liver inflow"), the hepatic vein (representing the "liver outflow"), and the renal vein (representing the "renal outflow") (18). Compared with control mice, the absence of liver GDH resulted in a marked elevation of plasma ammonia levels at any of the sites. Hep*Glud1*$^{-/-}$ mice showed mild systemic arterial hyperammonemia (+59%, $P < 0.01$), along with increased portal venous ammonia (+51%, $P < 0.05$) irrigating the liver (Fig. 2*A*). The similar differences observed between control and GDH-null mice in aorta and in portal vein indicate that the intestine did not contribute to the higher ammonia levels in Hep*Glud1*$^{-/-}$ mice (Fig. 2*A*). Hepatic ammonia metabolism was not sufficient to normalize the hepatic vein ammonia levels in Hep*Glud1*$^{-/-}$ mice, as revealed by the gap between control and Hep*Glud1*$^{-/-}$ mice, even more pronounced in this compartment (+117%, $P < 0.01$) (Fig. 2*A*). Sampling from the hepatic vein revealed that control *Glud1*$^{lox/lox}$ livers were able to clear 49% ($P < 0.01$) of the portal ammonia, a clearance that dropped to only 27% ($P = 0.07$) for Hep*Glud1*$^{-/-}$ livers (Fig. 2*A*). The resulting increased hepatic ammonia output in Hep*Glud1*$^{-/-}$ mice was further witnessed by the higher hepatic arteriovenous difference for ammonia (Fig. 2*B*). Moreover, the absence of GDH in the liver resulted in an increase of ammonia concentrations in renal venous plasma (+154%, $P < 0.01$) (Fig. 2*A*). We also observed a higher magnitude of the renal arteriovenous difference for ammonia (Fig. 2*B*), indicating increased renal ammonia output as a consequence of liver-specific GDH deletion. This observation was supported by increased GLS protein levels in kidney of Hep*Glud1*$^{-/-}$ mice (Supplementary Fig. 4*A*). Accordingly, we measured higher peripheral venous ammonia levels in Hep*Glud1*$^{-/-}$ mice (+93%, $P < 0.001$) (Fig. 2*C*). Finally, urine ammonia levels were higher in Hep*Glud1*$^{-/-}$ mice compared with controls (Fig. 2*D*).

In normal conditions, the liver detoxifies ammonia by synthesizing urea, which is then released in the blood and excreted by the kidneys before its elimination through urine (3,19). Peripheral venous urea levels were decreased in Hep*Glud1*$^{-/-}$ mice (−35%, $P < 0.001$) (Fig. 2*E*) due to reduced urea synthesis by the liver as shown by lower hepatic vein urea levels (−14%, $P < 0.05$) (Fig. 2*F*). As a consequence, urea levels measured in the urine of Hep*Glud1*$^{-/-}$ mice were much lower than those of control mice (−45%, $P < 0.01$) (Fig. 2*G*).

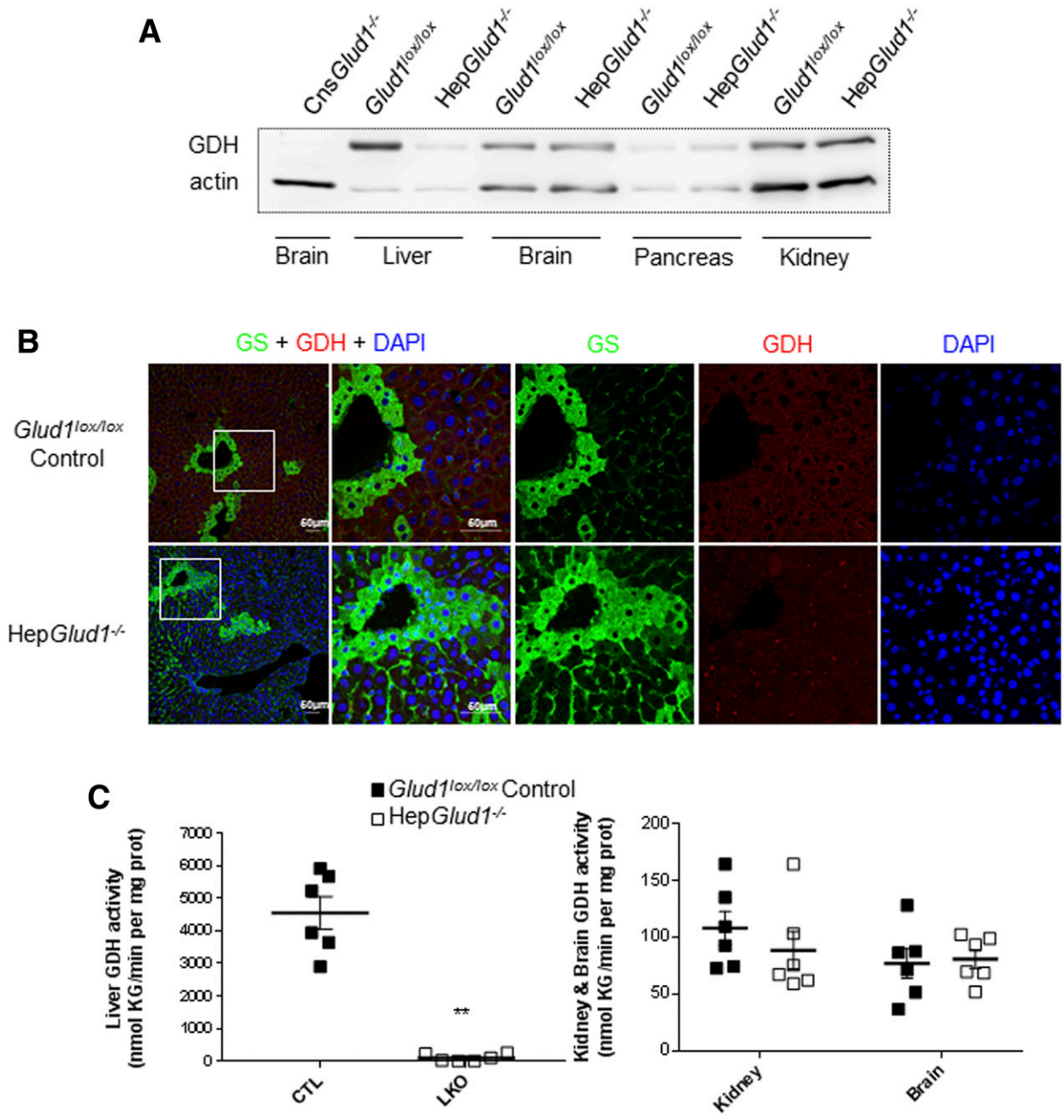

Figure 1—Assessment of liver-specific GDH-knockout mouse, Hep*Glud1*$^{-/-}$. *A*: Liver-specific GDH knockout was controlled by immunoblotting and compared with nonliver tissues collected from control (*Glud1*$^{lox/lox}$) and Hep*Glud1*$^{-/-}$ mice. Brain extracts from constitutive GDH brain knockout Cns*Glud1*$^{-/-}$ mice served as a negative control for GDH expression. Actin served as loading control. Immunoblots are representative of four independent preparations. *B*: Representative maximal projections of confocal images of liver cryosections from *Glud1*$^{lox/lox}$ control and Hep*Glud1*$^{-/-}$ mice costained for GDH (red), GS (green), and nuclei (DAPI, blue) ($n = 5$). *C*: Enzymatic oxidative activity of GDH measured in tissue extracts of *Glud1*$^{lox/lox}$ control (CTL) and Hep*Glud1*$^{-/-}$ (LKO) mice using glutamate as the substrate ($n = 6$). Values are means ± SEM. $^{**}P < 0.01$, *Glud1*$^{lox/lox}$ control vs. Hep*Glud1*$^{-/-}$ mice.

Because glutamate is required for ammonia removal systems, we measured the activities of liver enzymes involved in glutamate handling. In the fed state, protein levels of GS and enzymatic activities of GS, GLS, ASAT, and ALAT were similar between control and Hep*Glud1*$^{-/-}$ mice (Supplementary Fig. 4*B*–*F*). These data show that the lack of liver GDH was not compensated by other liver enzymes involved in glutamate handling.

Finally, glutamine and glutamate levels were similar in the livers of Hep*Glud1*$^{-/-}$ and control mice. However, aspartate levels were significantly decreased in the Hep*Glud1*$^{-/-}$ liver (Fig. 2*H*). The process of urea cycle involves equimolar provision of NH_3 and aspartate (20,21). Thus, the limiting step for urea synthesis in Hep*Glud1*$^{-/-}$ mice could be the availability of aspartate required in the urea cycle, leading to decreased

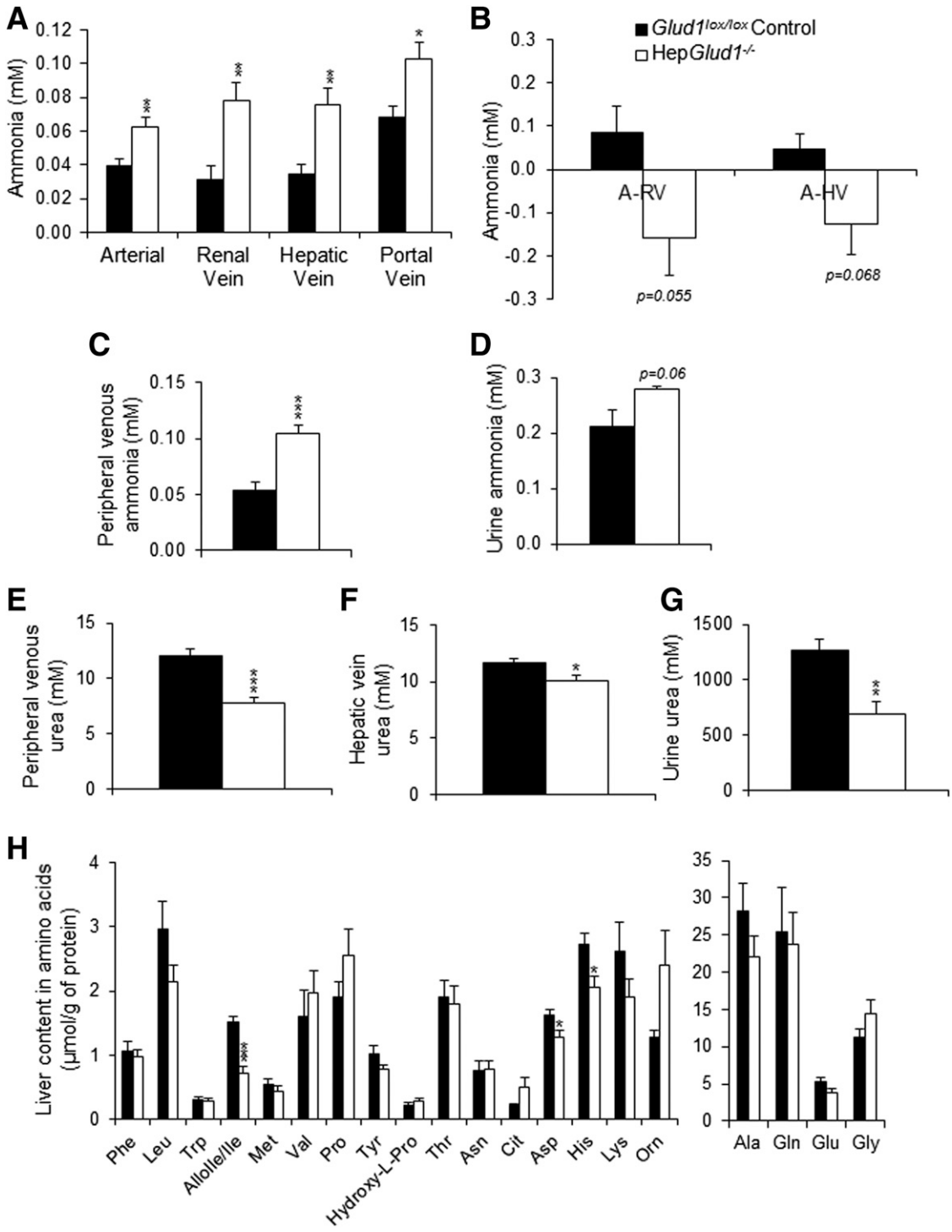

Figure 2— Lack of GDH in Hep*Glud1*$^{-/-}$ livers alters NH_3 handling. *A*: Plasma NH_3 levels were measured in the same mice at different sites: aorta (arterial), renal vein, hepatic vein, and portal vein (n = 6–8). *B*: Hepatic and renal arteriovenous differences for NH_3 in *Glud1*$^{lox/lox}$ control and Hep*Glud1*$^{-/-}$ mice (n = 8). A, arterial; HV, hepatic vein; RV, renal vein. *C*: Retro-orbital sampling allowed quantification of peripheral venous NH_3 levels (n = 8). *D*: Urine NH_3 levels (n = 6–8). Peripheral venous (*E*), hepatic vein (*F*), and urine urea (*G*) levels in *Glud1*$^{lox/lox}$ control and Hep*Glud1*$^{-/-}$ mice (n = 7–9). *H*: Liver content in amino acids (n = 5–6). All values are means ± SEM. *$P < 0.05$; **$P < 0.01$; ***$P < 0.001$, control vs. Hep*Glud1*$^{-/-}$ mice.

liver clearance of ammonia into urea. Upstream of aspartate incorporation, the hepatic contents of the urea cycle intermediates ornithine and citrulline were similar between controls and Hep*Glud1*$^{-/-}$ mice (Fig. 2*H*), indicating that these intermediates were not rate limiting.

Altogether, this set of data shows that the specific deletion of GDH in the liver alters ammonia homeostasis

due to increased ammonia output and decreased detoxification into urea.

Liver GDH Directs Rhythms of Feeding Behavior and Energy Substrate Utilization

Hep*Glud1*$^{-/-}$ mice showed similar body weight and body fat versus lean mass distribution compared with *Glud1*$^{lox/lox}$ controls (Fig. 3*A* and *B*). These parameters were conserved during lifetime (data not shown). Remarkably, the absence of liver GDH modified the food intake profile. Hep*Glud1*$^{-/-}$ mice exhibited a shift in their circadian rhythm of feeding: they stopped eating earlier at night, before the end of the dark cycle, and began eating earlier during the normal fasting daytime in the afternoon, way before the end of the light cycle (Fig. 3*C* and Supplementary Fig. 5). This was associated with a slight decrease in food intake over a 24-h period (Supplementary Fig. 5). Whereas the spontaneous locomotor activity tended to be lower in Hep*Glud1*$^{-/-}$ mice compared with *Glud1*$^{lox/lox}$ controls (Supplementary Fig. 6), the energy expenditure was similar between the two groups (Supplementary Fig. 7). The calculated VCO_2/VO_2 revealed a significant shift toward lower values in RER pointing to differential energy substrate

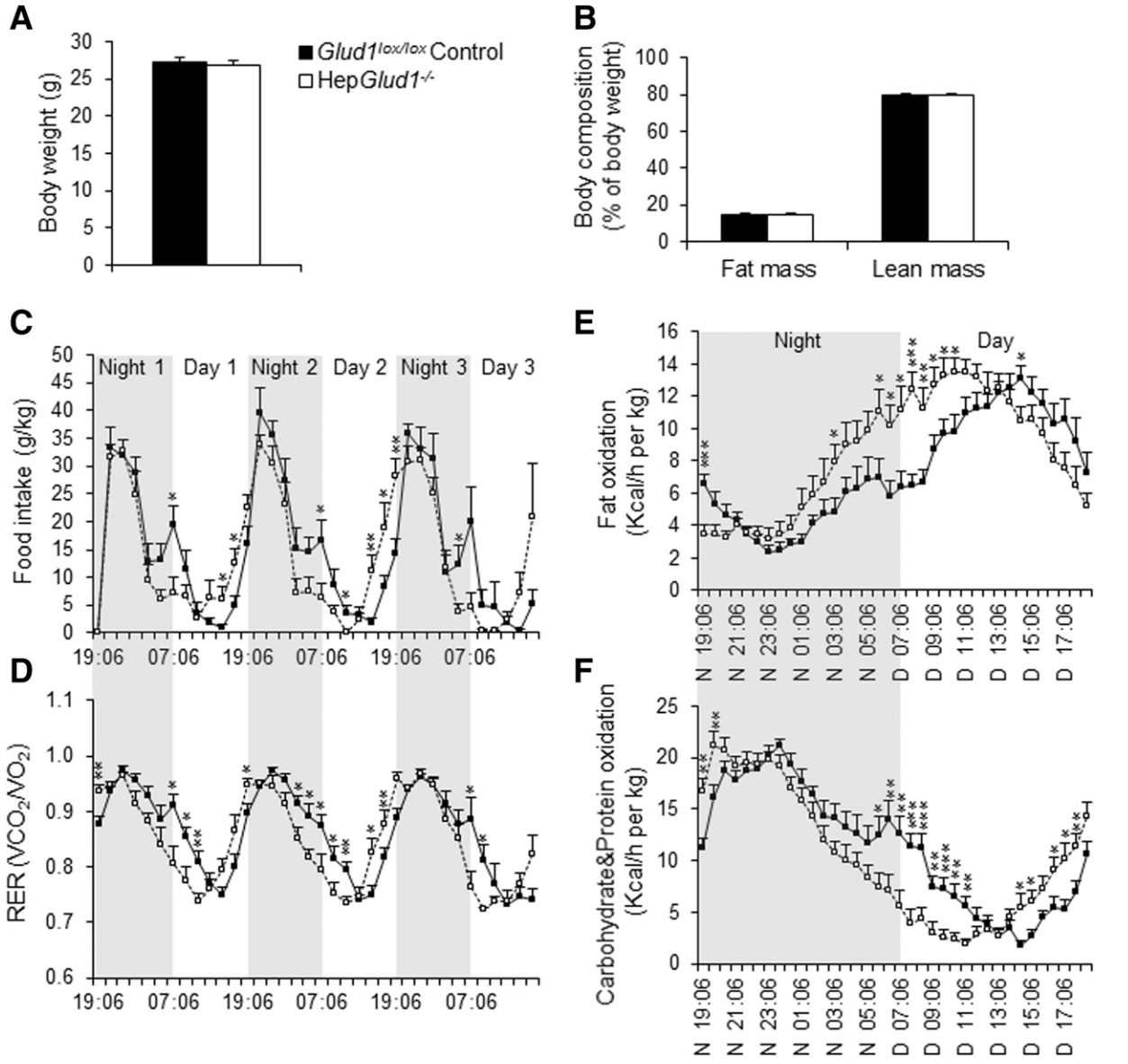

Figure 3—Altered food intake and early recruitment of lipids in Hep*Glud1*$^{-/-}$ mice. Body weight (*A*) and body composition (*B*) showing lean and fat mass distribution in *Glud1*$^{lox/lox}$ control and Hep*Glud1*$^{-/-}$ mice measured by EchoMRI (n = 9). Nonincremental food intake (*C*) and RER as VCO_2/VO_2 (*D*) measured over three consecutive 24-h periods composed of nighttime and daytime (n = 12). Extrapolated fat (*E*) and carbohydrate and protein oxidation (*F*) represented over a 24-h period corresponding to the mean of three consecutive periods of 24 h composed of nighttime (N) and daytime (D) (n = 12). All values are means ± SEM. *$P < 0.05$; **$P < 0.01$; ***$P < 0.001$, control vs. Hep*Glud1*$^{-/-}$ mice.

utilization (Fig. 3*D* and Supplementary Fig. 8). The calculated fat versus carbohydrate and protein oxidation (22) showed that at the whole-body level, lipids were favored over carbohydrates and proteins as energy fuel in Hep*Glud1*$^{-/-}$ mice compared with control animals (Fig. 3*E* and *F*).

The difference in feeding behavior between Hep*Glud1*$^{-/-}$ and *Glud1*$^{lox/lox}$ mice did not affect the glycemia measured in the morning in the fed state or after an O/N fasting-induced metabolic challenge (Fig. 4*A*). Even older (25–27 weeks of age) control *Glud1*$^{lox/lox}$ and knockout Hep*Glud1*$^{-/-}$ mice fasted for 24 h exhibited similar glycemia (3.8 ± 0.3 and 4.6 ± 0.3 mmol/L, respectively; n = 5–6). The first metabolic response to fasting is liver glycogenolysis. In the fed condition, deletion of GDH in the hepatocytes did not modify liver glycogen content that was efficiently restored upon feeding (Fig. 4*B*), without changes in the expression of glucokinase as assessed by immunoblotting (data not shown). Fasting-induced depletion of liver glycogen was similar between Hep*Glud1*$^{-/-}$ and *Glud1*$^{lox/lox}$ control animals, showing a rapid mobilization and nearly complete depletion (~98% drop) already after 6 h of fasting in both groups (Fig. 4*B*). Upon energy need, reduced blood insulin levels promote lipolysis of fat stored as triglycerides in adipose tissue leading to the release of free fatty acids (FFAs) used for β-oxidation, ketogenesis, and reformation of triglyceride-rich lipoproteins in the liver. Plasma FFA levels in the fed condition were similar in Hep*Glud1*$^{-/-}$ and *Glud1*$^{lox/lox}$ control animals (Fig. 4*C*). However, Hep*Glud1*$^{-/-}$ mice showed lower circulating levels of FFA in the fasting state compared with controls (Fig. 4*C*) despite similar insulin levels (Supplementary Table 1). The fasting-induced ketone body production was preserved in Hep*Glud1*$^{-/-}$mice (Fig. 4*D*). Higher clearance of plasma FFA is in line with the preferential utilization of lipids as energy substrates in Hep*Glud1*$^{-/-}$ mice.

Liver GDH Is Mandatory for Alanine-Induced Gluconeogenesis

Glucose tolerance tests revealed normal glucose excursions in Hep*Glud1*$^{-/-}$ animals (Fig. 5*A*), and insulin tolerance tests showed similar peripheral sensitivity in Hep*Glud1*$^{-/-}$ mice and *Glud1*$^{lox/lox}$ controls (Fig. 5*B*). Next, we investigated the gluconeogenic capacity of Hep*Glud1*$^{-/-}$ mice by measuring the rise in blood glucose after the i.p. administration of substrates recruited in situations of energy imbalance, such as fasting. Administration of glycerol or pyruvate, two GDH-independent gluconeogenic substrates, induced similar increases in blood glucose levels in knockout and control mice (Fig. 5*C* and *D*). Then we tested the GDH-dependent amino acids glutamine and

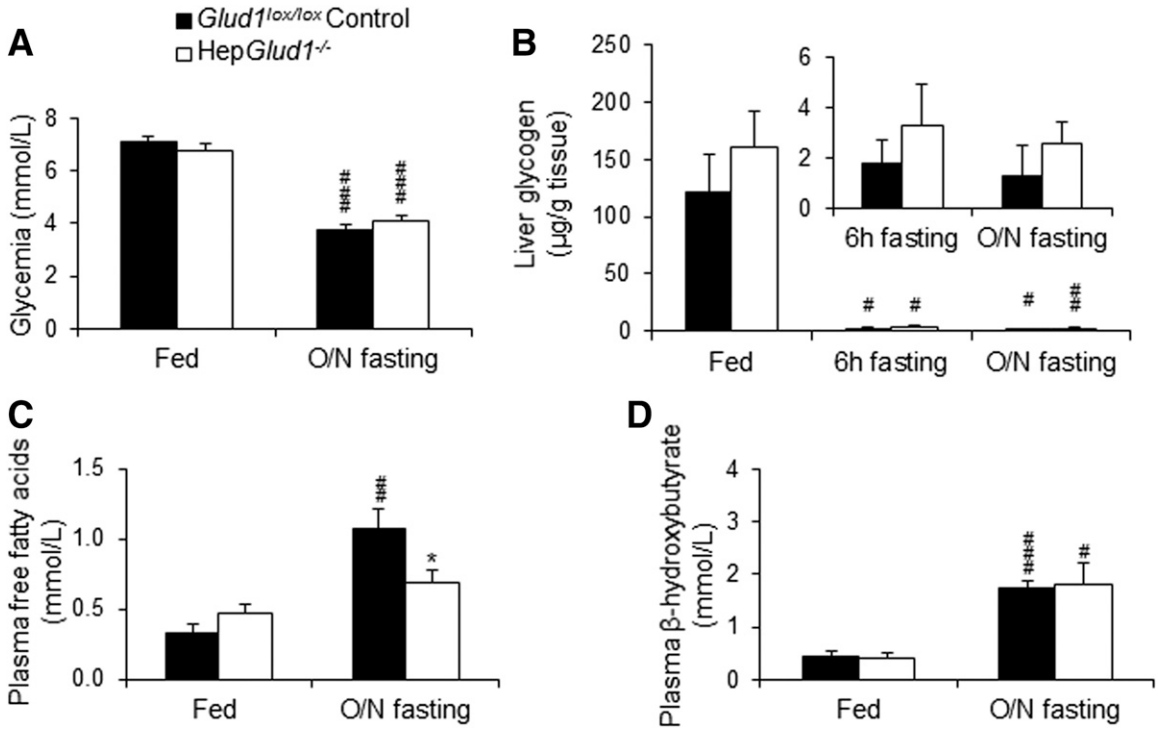

Figure 4—Lipid utilization is favored in Hep*Glud1*$^{-/-}$mice. *A*: Plasma glucose levels in fed and O/N-fasted *Glud1*$^{lox/lox}$ control and Hep*Glud1*$^{-/-}$ mice (n = 13–16). Liver glycogen content (the inset shows the 6 h and O/N fasting condition with adjusted scale) (*B*), plasma FFAs (*C*), and plasma β-hydroxybutyrate concentrations (*D*) in fed and O/N fasted *Glud1*$^{lox/lox}$ control and Hep*Glud1*$^{-/-}$ mice (n = 6–8). All values are means ± SEM. *$P < 0.05$, control vs. Hep*Glud1*$^{-/-}$ mice. #$P < 0.05$; ##$P < 0.01$; ###$P < 0.001$, fasting vs. fed condition of corresponding genotype.

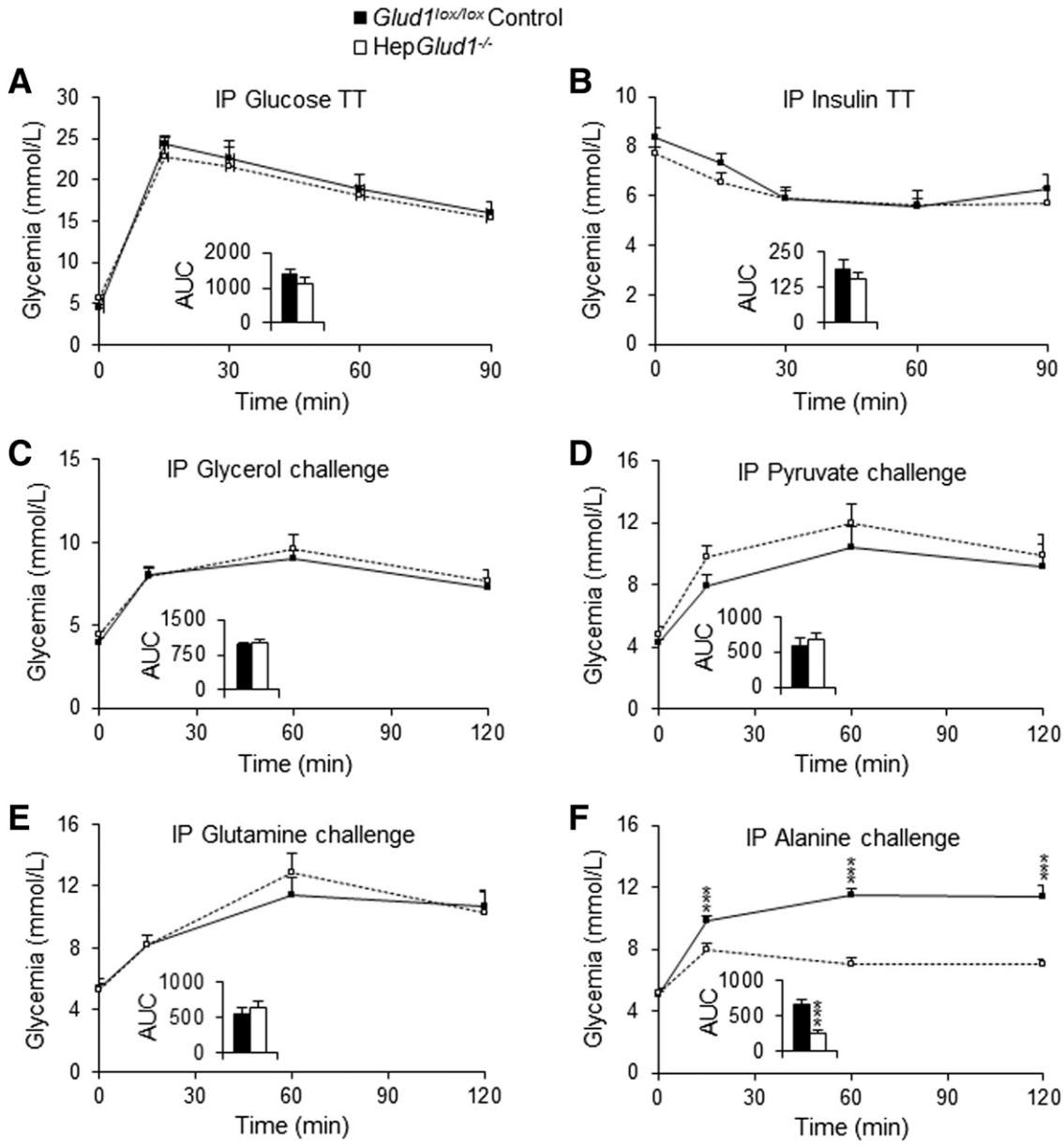

Figure 5—Alanine-induced gluconeogenesis is altered in Hep*Glud1*$^{-/-}$ mice. Glucose tolerance test (2 g/kg) (*A*) and insulin tolerance test (0.75 units/kg) (*B*) with corresponding area under the curve (AUC) in *Glud1*$^{lox/lox}$ control and Hep*Glud1*$^{-/-}$ mice (n = 6–8). Blood glucose levels in response to glycerol challenge (2 g/kg; n = 8–9) (*C*), pyruvate challenge (2 g/kg; n = 11–13) (*D*), glutamine challenge (2 g/kg; n = 10–13) (*E*), and alanine challenge (2 g/kg; n = 19–22) (*F*) with corresponding AUC in *Glud1*$^{lox/lox}$ control and Hep*Glud1*$^{-/-}$ mice. IP, intraperitoneal; TT, tolerance test. All values are means ± SEM. ***$P < 0.001$, control vs. Hep*Glud1*$^{-/-}$ mice.

alanine, two major substrates transported from the muscles during periods of active gluconeogenesis. Glycemia of control mice increased in response to both glutamine and alanine challenge (Fig. 5*E* and *F*). Of note, the CreER^{T2} transgene per se did not affect the alanine response (Supplementary Fig. 9*A*). Remarkably, glutamine was able to increase glycemia in Hep*Glud1*$^{-/-}$ mice, whereas the alanine response was markedly impaired in the absence of hepatic GDH (Fig. 5*F* and Supplementary Fig. 9). This effect observed 4 weeks after recombination (i.e., at 12 weeks of age) was preserved in older mice 17 weeks after recombination (Supplementary Fig. 9*B*). Because the skeletal muscles may contribute to the supply of gluconeogenic amino acids to the liver, we assessed the levels of such metabolites in soleus and gastrocnemius muscles, revealing no major differences between Hep*Glud1*$^{-/-}$ mice and *Glud1*$^{lox/lox}$ controls (Supplementary Fig. 10).

We then measured plasma amino acids in fed and O/N-fasted mice (Fig. 6*A* and *B* and Supplementary Fig. 11). Circulating glutamine levels were higher in fed Hep*Glud1*$^{-/-}$ mice compared with *Glud1*$^{lox/lox}$ controls (Fig. 6*A*).

Interestingly, plasma glutamine levels decreased after O/N fasting in Hep*Glud1*$^{-/-}$ mice but not in control animals (Fig. 6*A*), indicating an increased utilization of glutamine in Hep*Glud1*$^{-/-}$ mice. O/N fasting induced efficient clearance of plasma alanine in *Glud1*$^{lox/lox}$ control animals, which was not the case in Hep*Glud1*$^{-/-}$ mice (Fig. 6*B*).

Whereas gluconeogenesis from glutamine takes place in the kidneys and the intestine, gluconeogenesis from alanine and lactate is the key pathway in the liver (23). We thus tested the gluconeogenic capacity of isolated primary hepatocytes and renal proximal tubular cells. In control hepatocytes, alanine and glutamine stimulation increased glucose production compared with the basal state (Fig. 6*C*). However, hepatocytes isolated from Hep*Glud1*$^{-/-}$ mice failed to increase glucose production in response to alanine and glutamine, both being GDH-dependent substrates (Fig. 6*C*). In renal proximal tubule cells, only glutamine could promote glucose production to similar extents in both groups (Fig. 6*D*).

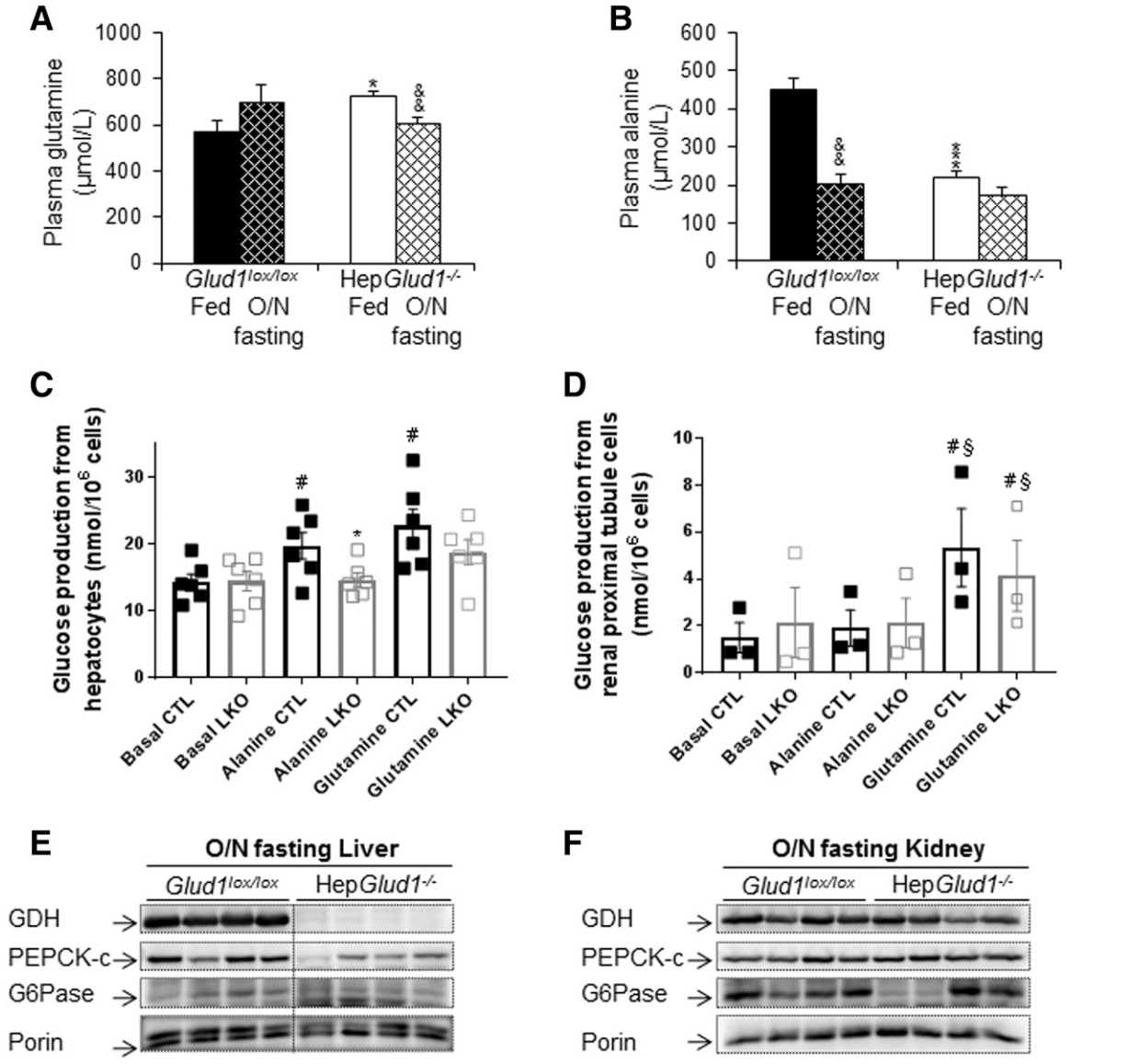

Figure 6—The kidney of Hep*Glud1*$^{-/-}$ mice does not compensate for altered liver gluconeogenesis. Plasma glutamine (*A*) and alanine (*B*) levels measured in fed and O/N fasting conditions ($n = 7$). Glucose production by primary hepatocytes (*C*) and renal proximal tubule cells (*D*) isolated from control *Glud1*$^{lox/lox}$ (CTL) and Hep*Glud1*$^{-/-}$ (LKO) mice in response to alanine and glutamine stimulations compared with incubation in basal medium (n = 3–6). Immunoblotting for liver (*E*) and kidney (*F*) GDH, PEPCK-c, and G6Pase in Hep*Glud1*$^{-/-}$ mice compared with *Glud1*$^{lox/lox}$ controls in O/N fasting state. All values are means ± SEM. *$P < 0.05$, ***$P < 0.001$, control vs. Hep*Glud1*$^{-/-}$ mice in the same fed or fasting state. &&$P < 0.01$, fasting vs. fed condition of corresponding genotype. #$P < 0.05$, amino acid stimulation compared with basal condition of corresponding genotype. §$P < 0.05$, glutamine stimulation compared with alanine stimulation of corresponding genotype.

In agreement with these data, the O/N fasting induced a robust gluconeogenic adaptive response in livers of *Glud1*$^{lox/lox}$ and Hep*Glud1*$^{-/-}$ mice, as shown by increased PEPCK-c and G6Pase protein levels (Supplementary Fig. 12). However, fasting-induced PEPCK-c upregulation was less efficient in liver of Hep*Glud1*$^{-/-}$ mice compared with *Glud1*$^{lox/lox}$ controls (Fig. 6*E*), not compensating for the impaired alanine-induced gluconeogenic activity in the knockout animals. In fasting kidney, no differences of PEPCK and G6Pase levels were observed between *Glud1*$^{lox/lox}$ and Hep*Glud1*$^{-/-}$ kidneys (Fig. 6*F* and Supplementary Fig. 12*A*). Consistently, both groups exhibited similar levels of amino acids in kidney extracts (Supplementary Fig. 12*B*).

Altogether, these data show altered gluconeogenesis in the liver of Hep*Glud1*$^{-/-}$ mice.

DISCUSSION

Urea synthesis and gluconeogenesis characterize some of the prominent liver functions, closely related to each other through amino acid metabolism. On one hand, deamination of the α-amino group of amino acids produces ammonia, a toxic metabolite that is detoxified by its conversion into urea via the ornithine cycle in the liver. On the other hand, carbon skeletons derived from deaminated amino acids are preferentially converted into glucose by gluconeogenic enzymes. The present in vivo study, using a liver-specific GDH-deficient mouse, shows that hepatic GDH is central to ammonia homeostasis and gluconeogenesis from amino acids. Regarding nitrogen metabolism, deletion of liver GDH triggered a systemic rise in ammonemia due to decreased detoxification into urea and to increased ammonia output (Fig. 7*A*).

Although GDH is found throughout the liver lobules, its activity increases from periportal to perivenous cells (24). Labeling experiments have confirmed the bidirectionality of the GDH pathway (25–28). In periportal hepatocytes expressing the urea cycle enzymes, where deamination of much of the amino acids takes place, GDH function is thought to be the deamination (29); whereas in perivenous hepatocytes, where GDH levels are particularly high, GDH may produce glutamate needed for glutamine synthesis via GS. In the liver, although glutamate deamination through GDH supplies nitrogen to the urea cycle in the form of ammonium, the reaction toward glutamate production may have multiple consequences on the regulation of systemic ammonia detoxification.

As formulated by Nissim et al. (30), the formation of glutamate from ammonia may *1*) serve as a scavenger for excess of ammonia; *2*) improve the availability of mitochondrial glutamate for the synthesis of *N*-acetylglutamate; and *3*) lead to the formation of aspartate via the ASAT reaction. Consequently, increased *N*-acetylglutamate and aspartate levels favor ammonia detoxification via urea synthesis. In Hep*Glud1*$^{-/-}$ mice, hepatic aspartate levels were reduced and might have contributed to the incomplete conversion of ammonia to urea, pointing to the liver as the primary source of the excess ammonia measured in the knockout animals. Of note, an alternative route to urea production for clearance of ammonia from the body is exhalation. Indeed, Hibbard and Killard (31) reported that excess ammonia not efficiently excreted out of the body may diffuse into the lungs and can be exhaled in breath. This was not assessed in the current study, and future studies with flux measurements might help delineating interorgan ammonia turnover in the absence of liver GDH.

In kidneys, GDH operates toward the deamination direction, thereby contributing to at least 25% of the renal ammonia production (32), the main proportion being produced by the deamidation of glutamine by the action of glutaminase. A study in rats showed that activation of GDH induced by β-2-aminobicyclo-(2.2.1)-heptane-2-carboxylic acid (BCH) resulted in increased ammonia production by the kidney (33). Under conditions of acidosis, a marked increase in glutamate deamination was found, with the GDH pathway contributing to approximately half of the augmented ammonia production (34). We did not find any upregulation of GDH protein or activity levels in the kidneys of Hep*Glud1*$^{-/-}$ mice. However, increased glutaminase levels in Hep*Glud1*$^{-/-}$ mice led to higher renal ammoniagenesis as measured by increased ammonia levels in the renal vein and urine.

We previously reported the important contribution of GDH to brain energy metabolism (35,36). The liver being one of the major organs contributing to metabolic control, we have now examined the putative importance of liver GDH for whole-body energy homeostasis in the Hep*Glud1*$^{-/-}$ mouse model. Although the body weight and body composition were similar between control and Hep*Glud1*$^{-/-}$ mice, the food intake profile and the RER were different between genotypes. In fact, the deletion of GDH in the liver led to modified recruitment of body fuel in Hep*Glud1*$^{-/-}$ mice, with preferential utilization of lipids over carbohydrates and proteins as energy substrates in the postprandial state. GDH participates to cataplerosis during periods of increased energy supply and to anaplerosis during periods of increased energy demand feeding the tricarboxylic acid cycle (11). The reaction catalyzed by GDH links carbohydrate to protein metabolism. At the whole-body level, the metabolic shift to fatty acid metabolism seems to be a compensatory mechanism for reduced carbohydrates/protein utilization in the absence of liver GDH and the subsequent impaired hepatic glucose production (Fig. 7*B*).

Fasting represents an important metabolic challenge. During fasting, the nutritional glucose supply becomes progressively limiting, glucose production being maintained through glycogen breakdown (glycogenolysis) and then de novo glucose synthesis (gluconeogenesis) upon starving conditions. Because proteolysis is mainly responsible for the net production of gluconeogenic precursors, oxidation of fatty acids is essential as an

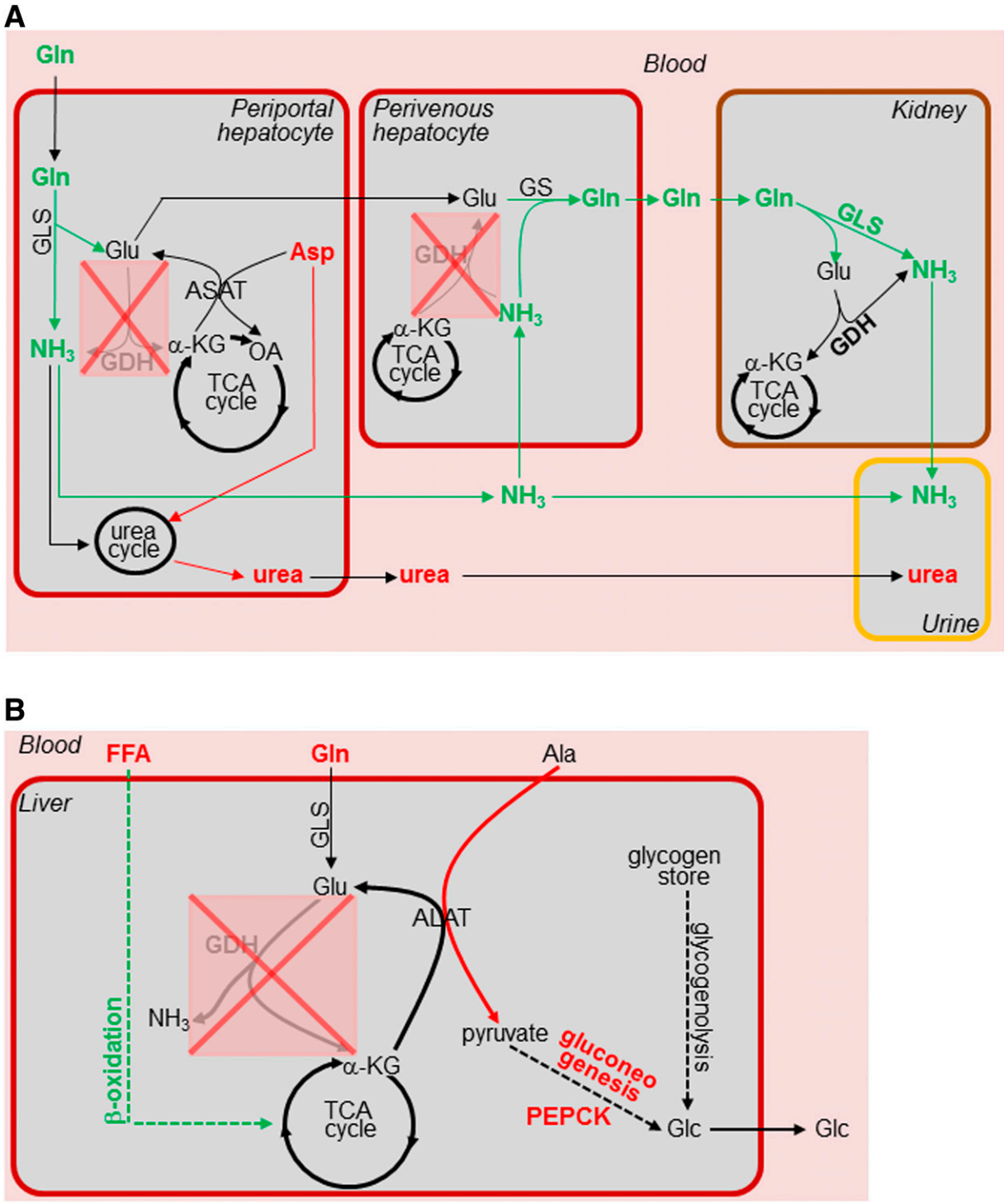

Figure 7—Scheme depicting the consequences of GDH deletion in the liver. *A*: NH_3 metabolism in Hep*Glud1*$^{-/-}$ mice in fed condition. *B*: Energy metabolism in Hep*Glud1*$^{-/-}$ mice in fasting condition. Pathways and metabolites increased in Hep*Glud1*$^{-/-}$ mice are shown in green, and the decreased ones are in red. OA, oxaloacetate; TCA, tricarboxylic acid cycle.

alternative pathway to prevent a rapid erosion of the protein mass (37,38). The contribution of glycogenolysis was similar in control versus knockout mice, whereas the lower circulating FFA levels in Hep*Glud1*$^{-/-}$ mice observed upon prolonged fasting was in line with increased fatty acid oxidation.

The importance of gluconeogenesis rapidly increases with the duration of fasting, exhaustion of the glycogen stores initiating starving conditions. When livers from fasted rats are perfused with a mixture of physiological gluconeogenic substrates at their normal plasma levels, amino acids account for more than 50% of the glucose

production (39). Most amino acids derived from proteins of the skeletal muscles are converted to alanine and glutamine and released in the circulation before their uptake and use by the liver and the kidney, respectively. In addition, lactate and glycerol are used to similar extents by both gluconeogenic organs. In vivo challenge with various gluconeogenic substrates and in vitro stimulation of primary hepatocytes isolated from control and Hep*Glud1*$^{-/-}$ animals showed that liver gluconeogenesis from amino acids was altered in Hep*Glud1*$^{-/-}$ mice. Although alanine is primarily used by the liver, glutamine is used by the kidney for gluconeogenesis (23), while we did not observe compensatory glucose production in renal cells isolated from Hep*Glud1*$^{-/-}$ mice. In the liver of Hep*Glud1*$^{-/-}$ mice, alanine-derived gluconeogenesis via ALAT was probably impaired because of a shortage of ALAT substrate α-KG resulting from the absence of GDH.

Interestingly, there was no compensatory increase of the gluconeogenic capacity of the kidney, as indicated by similar levels of PEPCK-c and G6Pase. Furthermore, primary tubule cells isolated from Hep*Glud1*$^{-/-}$ mice did not enhance glucose output upon glutamine stimulation, showing that the kidney did not compensate for decreased liver gluconeogenesis in our model. However, lower circulating plasma glutamine levels in fasting Hep*Glud1*$^{-/-}$ mice compared with controls indicate an increase in glutamine utilization, potentially contributed by intestine gluconeogenesis.

Overall, our data point to liver GDH as a key player in glucose and amino acid metabolism, participating in the control of the circadian rhythm of food intake. On one hand, GDH regulates ammonia homeostasis. On the other hand, GDH contributes to whole-body energy homeostasis due to its role *1*) in the metabolic shift between carbohydrates/protein oxidation versus fatty acid oxidation and *2*) in gluconeogenesis from amino acids.

Acknowledgments. The authors are grateful to Dr. P. Chambon and Dr. D. Metzger (L'Institut de Génétique et de Biologie Moléculaire et Cellulaire, Strasbourg) for sharing the SA-Cre-ER^{T2} mice. The authors thank Dr. J. Altirriba (University of Geneva) for his help with metabolic cages data analyses and Dr. R. Martin-del-Rio and Dr. J. Tamarit-Rodriguez (Complutense University of Madrid) for plasma amino acid analyses. The authors thank G. Chaffard, C. Vesin, and F. Visentin for expert technical assistance as well as Dr. T. Brun and Dr. E. Feraille for helpful discussions (University of Geneva). The authors thank Dr. J. Ivanisevic and her team (University of Lausanne) for amino acid analyses. The authors are grateful to Dr. G. Mithieux's laboratory for sharing G6Pase antibody and in particular to Dr. F. Rajas for helpful discussion (INSERM U855, Lyon, France).

Funding. This work was supported by Gertrude von Meissner-Stiftung Foundation and Fondation Ernst et Lucie Schmidheiny (to M.K.), the Machaon Foundation (to Y.E.), and Schweizerischer Nationalfonds zur Förderung der Wissenschaftlichen Forschung (#135704 and #146984 to P.M.).

Duality of Interest. No potential conflicts of interest relevant to this article were reported.

Author Contributions. M.K., J.M.-L., M.G., L.L., E.D., and Y.E. performed research. M.K., Y.E., and P.M. analyzed data. M.K. and P.M. designed research and wrote the paper. P.M. is the guarantor of this work and, as such, has access to all the data in the study and takes responsibility for the integrity of the data and the accuracy of the data analysis.

Prior Presentation. Part of the study was presented at the 52nd Annual Meeting of the European Association for the Study of Diabetes, Munich, Germany, 12–16 September 2016.

References

1. Wright G, Noiret L, Olde Damink SW, Jalan R. Interorgan ammonia metabolism in liver failure: the basis of current and future therapies. Liver Int 2011;31:163–175

2. Aikawa T, Matsutaka H, Yamamoto H, Okuda T, Ishikawa E. Gluconeogenesis and amino acid metabolism. II. Inter-organal relations and roles of glutamine and alanine in the amino acid metabolism of fasted rats. J Biochem 1973;74:1003–1017

3. Haüssinger D. Nitrogen metabolism in liver: structural and functional organization and physiological relevance. Biochem J 1990;267:281–290

4. Nurjhan N, Bucci A, Perriello G, et al. Glutamine: a major gluconeogenic precursor and vehicle for interorgan carbon transport in man. J Clin Invest 1995;95:272–277

5. Rui L. Energy metabolism in the liver. Compr Physiol 2014;4:177–197

6. Sharabi K, Tavares CD, Rines AK, Puigserver P. Molecular pathophysiology of hepatic glucose production. Mol Aspects Med 2015;46:21–33

7. Donovan CM, Sumida KD. Training improves glucose homeostasis in rats during exercise via glucose production. Am J Physiol 1990;258:R770–R776

8. Burelle Y, Fillipi C, Péronnet F, Leverve X. Mechanisms of increased gluconeogenesis from alanine in rat isolated hepatocytes after endurance training. Am J Physiol Endocrinol Metab 2000;278:E35–E42

9. Wasserman DH, Cherrington AD. Hepatic fuel metabolism during muscular work: role and regulation. Am J Physiol 1991;260:E811–E824

10. Young VR. Nutrient interactions with reference to amino acid and protein metabolism in non-ruminants; particular emphasis on protein-energy relations in man. Z Ernahrungswiss 1991;30:239–267

11. Karaca M, Frigerio F, Maechler P. From pancreatic islets to central nervous system, the importance of glutamate dehydrogenase for the control of energy homeostasis. Neurochem Int 2011;59:510–517

12. Mallet LE, Exton JH, Park CR. Control of gluconeogenesis from amino acids in the perfused rat liver. J Biol Chem 1969;244:5713–5723

13. Stanley CA, Fang J, Kutyna K, et al. Molecular basis and characterization of the hyperinsulinism/hyperammonemia syndrome: predominance of mutations in exons 11 and 12 of the glutamate dehydrogenase gene. HI/HA Contributing Investigators. Diabetes 2000;49:667–673

14. Grimaldi M, Karaca M, Latini L, Brioudes E, Schalch T, Maechler P. Identification of the molecular dysfunction caused by glutamate dehydrogenase S445L mutation responsible for hyperinsulinism/hyperammonemia. Hum Mol Genet 2017;26:3453–3465

15. Carobbio S, Frigerio F, Rubi B, et al. Deletion of glutamate dehydrogenase in beta-cells abolishes part of the insulin secretory response not required for glucose homeostasis. J Biol Chem 2009;284:921–929

16. Schuler M, Dierich A, Chambon P, Metzger D. Efficient temporally controlled targeted somatic mutagenesis in hepatocytes of the mouse. Genesis 2004;39:167–172

17. Carobbio S, Ishihara H, Fernandez-Pascual S, Bartley C, Martin-Del-Rio R, Maechler P. Insulin secretion profiles are modified by overexpression of glutamate dehydrogenase in pancreatic islets. Diabetologia 2004;47:266–276

18. Ghallab A, Cellière G, Henkel SG, et al. Model-guided identification of a therapeutic strategy to reduce hyperammonemia in liver diseases. J Hepatol 2016;64:860–871

19. Adeva MM, Souto G, Blanco N, Donapetry C. Ammonium metabolism in humans. Metabolism 2012;61:1495–1511

20. Meijer AJ, Lamers WH, Chamuleau RA. Nitrogen metabolism and ornithine cycle function. Physiol Rev 1990;70:701–748

21. Yang D, Hazey JW, David F, et al. Integrative physiology of splanchnic glutamine and ammonium metabolism. Am J Physiol Endocrinol Metab 2000; 278:E469–E476
22. Bruss MD, Khambatta CF, Ruby MA, Aggarwal I, Hellerstein MK. Calorie restriction increases fatty acid synthesis and whole body fat oxidation rates. Am J Physiol Endocrinol Metab 2010;298:E108–E116
23. Stumvoll M, Meyer C, Perriello G, Kreider M, Welle S, Gerich J. Human kidney and liver gluconeogenesis: evidence for organ substrate selectivity. Am J Physiol 1998;274:E817–E826
24. Maly IP, Sasse D. Microquantitative analysis of the intra-acinar profiles of glutamate dehydrogenase in rat liver. J Histochem Cytochem 1991;39:1121–1124
25. Cooper AJ, Nieves E, Coleman AE, Filc-DeRicco S, Gelbard AS. Short-term metabolic fate of [^{13}N]ammonia in rat liver in vivo. J Biol Chem 1987;262:1073–1080
26. Cooper AJ, Nieves E, Rosenspire KC, Filc-DeRicco S, Gelbard AS, Brusilow SW. Short-term metabolic fate of ^{13}N-labeled glutamate, alanine, and glutamine(amide) in rat liver. J Biol Chem 1988;263:12268–12273
27. Brosnan JT, Brosnan ME, Charron R, Nissim I. A mass isotopomer study of urea and glutamine synthesis from 15N-labeled ammonia in the perfused rat liver. J Biol Chem 1996;271:16199–16207
28. Nissim I, Brosnan ME, Yudkoff M, Brosnan JT. Studies of hepatic glutamine metabolism in the perfused rat liver with (15)N-labeled glutamine. J Biol Chem 1999;274:28958–28965
29. Brosnan ME, Brosnan JT. Hepatic glutamate metabolism: a tale of 2 hepatocytes. Am J Clin Nutr 2009;90:857S–861S
30. Nissim I, Horyn O, Luhovyy B, et al. Role of the glutamate dehydrogenase reaction in furnishing aspartate nitrogen for urea synthesis: studies in perfused rat liver with 15N. Biochem J 2003;376:179–188
31. Hibbard T, Killard AJ. Breath ammonia levels in a normal human population study as determined by photoacoustic laser spectroscopy. J Breath Res 2011;5: 037101
32. van de Poll MC, Soeters PB, Deutz NE, Fearon KC, Dejong CH. Renal metabolism of amino acids: its role in interorgan amino acid exchange. Am J Clin Nutr 2004;79:185–197
33. Treberg JR, Clow KA, Greene KA, Brosnan ME, Brosnan JT. Systemic activation of glutamate dehydrogenase increases renal ammoniagenesis: implications for the hyperinsulinism/hyperammonemia syndrome. Am J Physiol Endocrinol Metab 2010;298:E1219–E1225
34. Schoolwerth AC, Nazar BL, LaNoue KF. Glutamate dehydrogenase activation and ammonia formation by rat kidney mitochondria. J Biol Chem 1978;253: 6177–6183
35. Karaca M, Frigerio F, Migrenne S, et al. GDH-dependent glutamate oxidation in the brain dictates peripheral energy substrate distribution. Cell Rep 2015;13: 365–375
36. Frigerio F, Karaca M, De Roo M, et al. Deletion of glutamate dehydrogenase 1 (Glud1) in the central nervous system affects glutamate handling without altering synaptic transmission. J Neurochem 2012;123:342–348
37. Cahill GF Jr. Starvation in man. N Engl J Med 1970;282:668–675
38. Cahill GF Jr. Fuel metabolism in starvation. Annu Rev Nutr 2006;26:1–22
39. Exton JH, Park CR. Control of gluconeogenesis in liver. I. General features of gluconeogenesis in the perfused livers of rats. J Biol Chem 1967;242:2622–2636